



FACILITY FORM 802

N65-82315	(THRU)
(ACCESSION NUMBER)	None
27	(CODE)
(PAGES)	
CP.60959	(CATEGORY)
(NASA CR OR TMX OR AD NUMBER)	

JET PROPULSION LABORATORY  
CALIFORNIA INSTITUTE OF TECHNOLOGY  
PASADENA, CALIFORNIA

**National Aeronautics and Space Administration**  
**Contract No. NASw-6**

**Technical Report No. 32-97**

**THE DETERMINATION OF NOISE**  
**TEMPERATURES OF**  
**LARGE ANTENNAS**

**D. Schuster**  
**C. T. Stelzried**  
**G. S. Levy**

**JET PROPULSION LABORATORY**  
**California Institute of Technology**  
**Pasadena, California**  
**May 1, 1961**

Copyright © 1961  
Jet Propulsion Laboratory  
California Institute of Technology

## ABSTRACT

The Jet Propulsion Laboratory has recently installed and tested masers at 960 and 2388 mc on an 85-ft paraboloidal antenna. This study was performed to determine system noise temperatures in future space-communication missions. Several low-noise feed configurations were evaluated. This evaluation required the development of techniques for the measurement of absolute noise temperatures. Liquid helium and nitrogen cooled loads were developed and evaluated.

Several receiver configurations were measured, and the techniques used and results obtained are discussed.

## THE DETERMINATION OF NOISE TEMPERATURES OF LARGE ANTENNAS\*

D. Schuster  
C. T. Stelzried  
G. S. Levy

The ultimate sensitivity limitation of any radio-reception system is determined by its noise temperature. In the past, receiver temperatures had been so high that the thermal contribution of all other components in the system could be ignored. With the advent of masers and parametric amplifiers, this is no longer the case. It is now quite possible to have a receiver system in which the thermal power from the antenna, circulator, and transmission lines is greater than that produced by the amplifier. In a low-noise reception system, therefore, one must know not only the receiver temperature but the antenna temperature as well.

The antenna temperature is defined as the temperature at which an equivalent resistor will produce the same thermal power as the antenna. The noise power produced by a resistor is given by

$$P = kTB$$

where  $k$  is Boltzmann's constant,  $T$  is absolute temperature, and  $B$  is the bandwidth. Thermal radiators which give rise to antenna temperatures are galactic background, discrete celestial sources (Ref. 1), ionosphere, atmosphere, Earth, and man-made interference. In addition to remote sources, resistive copper losses also produce thermal power.

---

\*This paper presents the results of one phase of research carried out at the Jet Propulsion Laboratory, California Institute of Technology, under Contract NASw-6, sponsored by the National Aeronautics and Space Administration.

If a paraboloidal antenna received energy only in the direction of its main beam, then, in the zenith position, it would see only the cold sky. Unfortunately, all antennas have side and back lobes, so that the thermal radiation from the Earth is the most serious spurious power source.

An experimental program has been underway at the Jet Propulsion Laboratory to determine the absolute antenna temperatures. This has led to a quantitative understanding of the origin of antenna noise and has resulted in the design of lower-noise configurations. Minimization of antenna temperature will result in improved performance of space-communication systems.

The JPL/NASA Deep Space Instrumentation Facility (DSIF) consists primarily of four 85-ft-diameter antennas located in California, Australia, and South Africa. The function of the net is to track, receive telemetry, and provide a command capability for space probes at planetary distances. The effectiveness of one of the large antennas may be described by a figure of merit derived from the one-way transmission equation, as follows:

$$P_R = P_T \frac{G_R G_T}{\left(\frac{4\pi r}{\lambda}\right)^2}$$

where

$P_R, P_T$  = received and transmitted power levels

$G_R, G_T$  = receiver and transmitter antenna gains

$r$  = range

$\lambda$  = wavelength

Since  $G = 4\pi A_e/\lambda^2$ , one can write

$$P_R = \frac{P_T}{\lambda^2} \frac{A_{eR} A_{eT}}{r^2}$$

where  $A_e$  = antenna effective area.

At the receiver threshold, one can set

$$P_R \simeq kT_S B$$

where  $T_S$  = system excess temperature at receiver input. Then,

$$kT_S B \simeq \frac{P_T}{\lambda^2} \frac{A_{eR} A_{eT}}{r^2}$$

or

$$\frac{4\pi k}{P_T A_{eT}} B r^2 \simeq \frac{4\pi A_{eR}}{\lambda^2 T_S} = M_R$$

where  $M_R$  = a figure of merit for the receiving antenna.

An improvement in the figure of merit of a receiving antenna can be translated into increased bandwidth or range capability.

The system excess temperature  $T_S$  has contributions from the antenna  $T_A$ , from resistive losses  $T_L$ , and from the receiving system  $T_R$ . Usually, reductions in all three contributions can be achieved.

$$M_R = \frac{\frac{4\pi A_{eR}}{\lambda^2}}{T_A + T_L + T_R} = \frac{G_R}{T_A + T_L + T_R}$$

Table 1 lists some measured values pertinent to figure-of-merit considerations. If a simple horn is used as a feed for the antenna, plots may be made of various parameters, as in Fig. 1, of figure of merit vs antenna temperature. These may be of use in determining the value of various improvements in the receiving system or in the transmission line.

Improvements can be made on a simple horn feed, however. The shaped beam feed mentioned in the last column of Table 1 is shown in Fig. 2. The ground plane and surface wave structure on the outer edge are effective in reducing the unwanted wide angle and backlobe radiation. The feed radiator is a simple, small-aperture, square horn. The symmetry of the device allows it to operate equally well with circular or linear polarization.

Simple improvements in the transmission line can be obtained by using the largest size rigid coaxial line suitable at the operating frequency or by using waveguide (see Fig. 3). Each component of the transmission line should be well matched with high-quality flat (lapped) and pinned connectors for measurement repeatability. Figure 4 shows the excess temperature that may be contributed by a mismatch at a single flange. This problem may be avoided if a four-port circulator is used with the port prior to the antenna line terminated in a cooled load. In the present case, the circulator is radiating ambient temperature noise toward the antenna. Last, the transmission line should be as short as possible.



The optimum transmission line might be obtained by having the maser attached to the feed horn. Otherwise, the line should be kept short, might be cooled to some degree, and circular guide might be used operating in the low-loss  $TE_{01}$  mode.

Improvements in the antenna and feed system, transmission line, and maser receiver should make it possible to achieve a 15 to 20°K system temperature with a large, paraboloidal reflector antenna. This would mean an improvement of 5 or 6 db in figure of merit over the present system.

An extensively used system for temperature measurements originally applied to radio astronomy by Dicke (Ref. 2) is shown in Fig. 5. The receiver noise is the same in both positions of the switch, so that changes in this noise do not appear on the record. This results in a decrease in sensitivity to receiver-gain changes. A temperature reference and calibration can be obtained by switching from the antenna to another load whose temperature can be varied (Ref. 3).

A null-type system developed by Ryle and Vonberg (Ref. 4) is shown in Fig. 6. System non-linearity is cancelled out with this technique. Usually, the antenna temperature is low (approximately 14°K for the JPL 2388-mc feed system), so that a cooled load and a variable attenuator are required for the variable noise source.

Several problems are encountered with rapidly switching-type radiometers. One is the impedance transient during the switching operation. This can cause receiver-gain changes, with consequent inaccuracy. Another problem is providing an equal match for both the load and antenna as seen by the receiver through the switch.

The first technique used for an absolute temperature measurement to evaluate the JPL HA-DEC receiver-site 960-mc antenna feed system in September 1960 is

shown in Fig. 7. The switching was done by hand. An extra circulator (external to the maser package) is used to increase the isolation of the maser amplifier from impedance changes caused by switching. The Hewlett Packard model 340B noise figure meter (NFM) used in the automatic mode of operation stabilizes the gain by application of an AGC voltage to an internal IF amplifier. The output of the NFM to the recorder is proportional to the power ratio obtained when the noise source is fired and not fired.

The antenna temperature is obtained by recording the output of the NFM when the maser is connected to the antenna, after first calibrating by connecting to the cooled termination through the various attenuators. If the reference termination is colder than the antenna, it is possible to add attenuation here rather than to the antenna. This results in a lower system temperature and greater accuracy. The recorded temperatures bracket the actual antenna temperature. It is possible to switch loads with a repeatability of about  $1^{\circ}\text{K}$ . The recorded temperatures are interpolated with an accuracy believed to be about  $2^{\circ}\text{K}$ . With the 960-mc 10-db taper horn, a temperature of  $29^{\circ}\text{K}$  is obtained when the antenna is pointed at the zenith. This includes about  $4^{\circ}\text{K}$  of resistive loss in the feed system.

Figure 8 shows a sketch of the liquid helium dewar. This  $1/3$ -liter-capacity portable (20 lb when fully loaded) dewar will maintain the termination at liquid helium temperature ( $4.2^{\circ}\text{K}$ ) for approximately 6 hr of active use between refills. The specially modified stoddart termination is submerged in the liquid helium. The actual equivalent noise temperature can be determined from measurements of the temperature distribution along the line and the insertion loss of the line as a function of temperature. These parameters are plotted in Figs. 9 and 10. The equivalent

noise temperature is calculated by dividing the line into sections, each with an associated temperature and insertion loss (Ref. 5). The resultant equivalent noise temperature for this load is plotted in Fig. 11 as a function of liquid helium level. Figure 12 shows a plot of VSWR vs frequency for the cooled coaxial termination.

The variable attenuation was obtained by the use of stainless-steel coaxial lines, as shown in Fig. 13. These units (1-, 2-, and 3-ft-length sections), with 1/2-in. -OD outer conductor and 3/16-in. -OD inner conductor, were constructed from commercial 0.035-in. -wall stainless-steel tubing. The VSWR of these attenuators is less than 1.04 at 960 mc, and the attenuation is 0.13 db/ft. When connected to a liquid helium cooled termination of 6.5°K, a 0.13-db attenuator at 280°K will contribute an excess noise temperature of 8.0°K to give a total equivalent noise temperature of 14.5°K.

Figure 14 shows a block diagram of the technique used for the evaluation of the JPL receiver-site 2388-mc feeds in February 1961. Temperature calibration is obtained by recording the system noise level when switched to the reference temperature, with the noise source fired and not fired. The noise level when switched to the antenna is interpolated from the recording. The measured equivalent noise temperature of the antenna with the 2388-mc feed used for the Venus radar experiment was about 14°K.

Some refinements were added to the liquid helium cooled termination. A larger dewar provided over 24 hr of continuous operation between refills. A standard EIA 7/8-in. flange connector was used at the upper end of the 3/4-in. -diameter stainless-steel gold-plated transmission line. The measured temperature distribution along the coaxial line and the insertion loss as a function of temperature are

shown in Figs. 15 and 16. The temperature distribution was made independent of the liquid helium level by providing a jacket of copper around the outer conductor and inside the inner conductor of the coaxial line. The equivalent temperature was calculated and found to be  $5.5^{\circ}\text{K}$  at the upper end of the transmission line.

The 2388-mc mixer and IF amplifier designed for low noise and high gain stability are shown in Fig. 17. The characteristics of this mixer are 4-mc bandwidth and 5-db single-channel noise (as seen looking into the filter). The cavity filter reduces the image and harmonic response of the mixer. The circulator is included to reduce the effect of slight mismatch on the amplifier gain when switching between the cooled termination and antenna.

The system gain stability must be better than 0.1% during the time of the measurement in order to have a measurement repeatability of about  $1^{\circ}\text{K}$ . This requires stabilized power supplies and good construction techniques of the mixer and IF amplifier. A 1% gain change is given by approximately 0.1% filament voltage change and 0.2% B-supply voltage change. Figure 18 shows a sample recording of the detected noise level of this amplifier after mounting at the focal point of the antenna. Here the peak-to-peak jitter is about  $2^{\circ}\text{K}$ , but the drift over the period of the recording is less than  $0.2^{\circ}\text{K}$ .

The 2388-mc mixer was used to evaluate the excess noise of the Bendix TD40 argon noise source. This source was also used as a standard noise source for the Venus radar experiment. A block diagram of the equipment is shown in Fig. 19. The circulator is used to reduce the gain change of the amplifier caused by switching loads. This was checked by switching between mismatched loads with a VSWR of

1.04 and 1.50. The gain change was not measurable with the recording system. The second and third harmonic responses were below 25 db. A typical recording showing the stability obtainable with this system is shown in Fig. 20. The increase in signal level is obtained when the noise source is fired. Repeatability is indicated by how well the signal returns to the original level. The effect of gas-tube current instability is shown to be small by the indicated variations in signal level with tube current. The actual measurement technique consisted of setting equal readings on the recorder with the precision attenuator. Calibration is obtained by measuring the power ratio between the cooled and ambient loads. The excess noise is then obtained from the power ratio between the cooled load with the noise source on and off.

A nonsynchronous type of radiometer with an absolute temperature-reference capability was set up at the JPL receiver site using the 2388-mc maser and the mixer, as shown in Fig. 21. The operating parameters are:

Center frequency	2388 mc
Bandwidth	2 mc
System temperature	80° K

The waveguide attenuator can be set to obtain a calibrating pulse when the noise source is turned on.

Figure 22 is a drift curve of Venus. This was obtained by setting the antenna at the declination of the source and approximately 1/2 deg ahead in hour angle. Venus then drifted through the antenna beam. This type of drift curve yields the change in antenna temperature produced by a source of a relative temperature of 0.45° K above the background.

Figure 23 is an absolute determination of the antenna temperature. The recording begins and ends on the helium load. An  $11^{\circ}\text{K}$  noise pulse is used to calibrate the scale. The effective temperature of the helium load at the waveguide switch is  $10^{\circ}\text{K}$ . After calibration on the helium load, the antenna is switched on and the noise pulse is repeated. This checks both linearity and gain stability of the system. (Other linearity tests are also employed.) The base line of the drift curve indicates that the effective antenna temperature at the switch is  $19^{\circ}\text{K}$  with this antenna orientation. A drift curve is then produced by M87 passing through the main beam. This causes an  $11^{\circ}\text{K}$  increase for a total absolute antenna temperature of  $30^{\circ}\text{K}$ . The system is then recalibrated on the antenna and helium load with noise pulses.

For radio-astronomical purposes, the relative temperature is generally adequate. However, for computation of figure of merit it is essential to have a value of the absolute antenna temperature (see Refs. 6 and 7).

Table 1. Measured system parameters

	960 mc		2388 mc		
	Feed with 14-db taper	Feed with 10-db taper	Feed with 14-db taper	Feed with 10-db taper	Shaped beam feed
$G_R$ , db	45.0	46.0	52.7	52.4	53.5
$T_A$ , °K	17	25	16	30	14
$T_L$ , °K	9	9	8	8	8
$T_R$ , °K	39	39	34	34	34
$T_S$ , °K	65	73	58*	72*	56
$M_R$ , db	+26.9	+27.4	+35.1	+33.8	+36.0

\*Estimated.

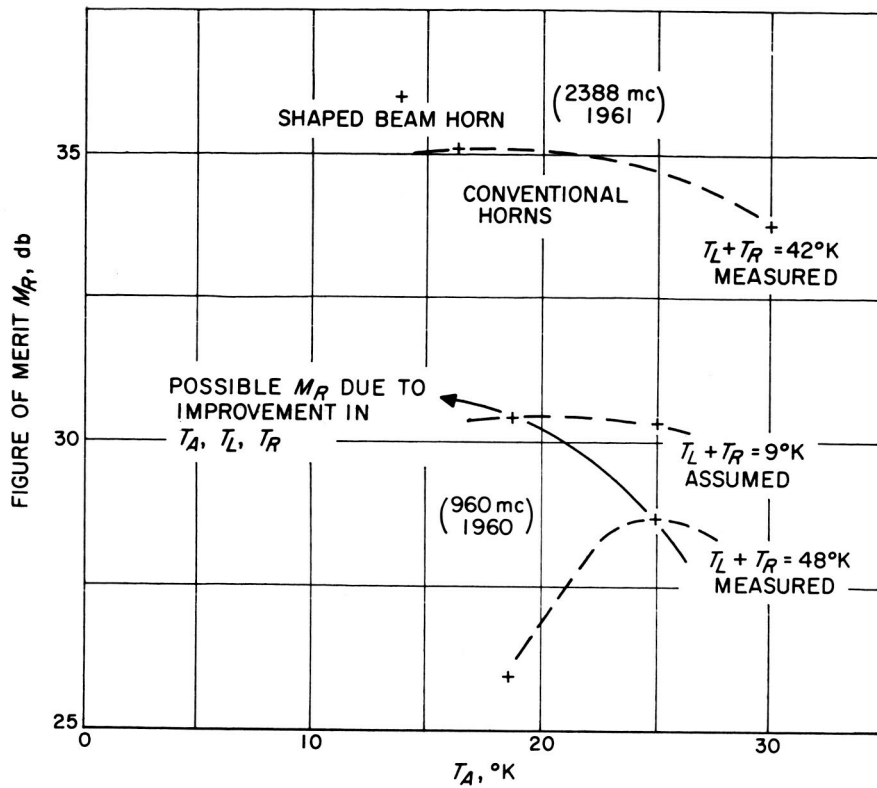
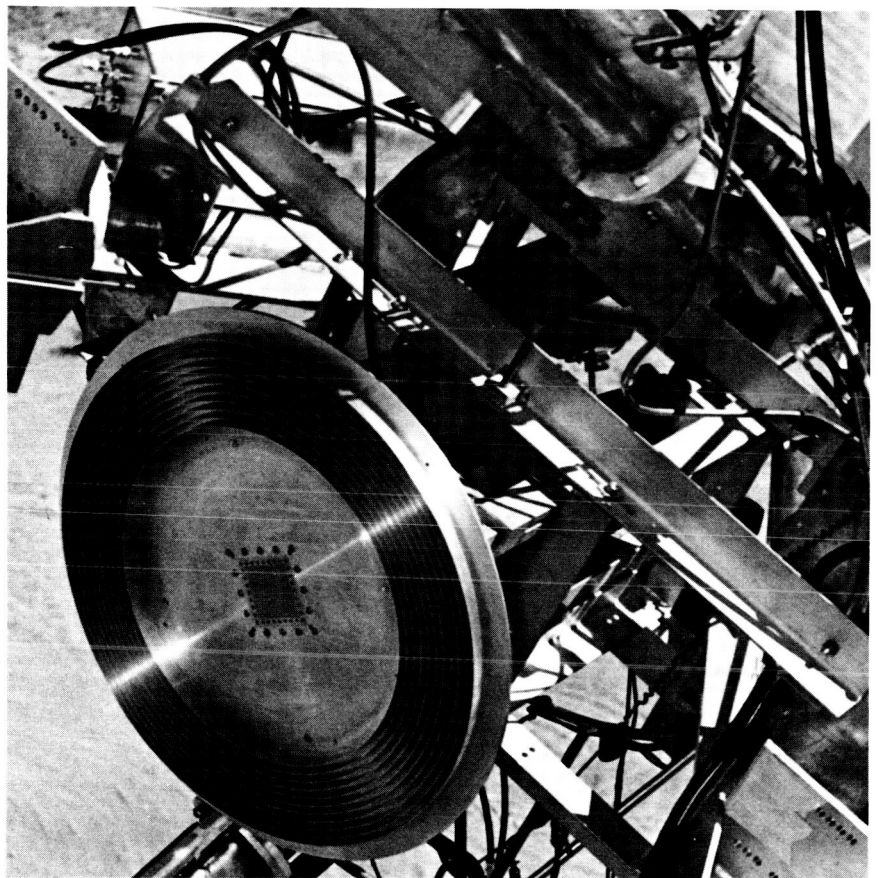


Fig. 1. Figure of merit vs antenna temperature

Fig. 2. Shaped beam feed





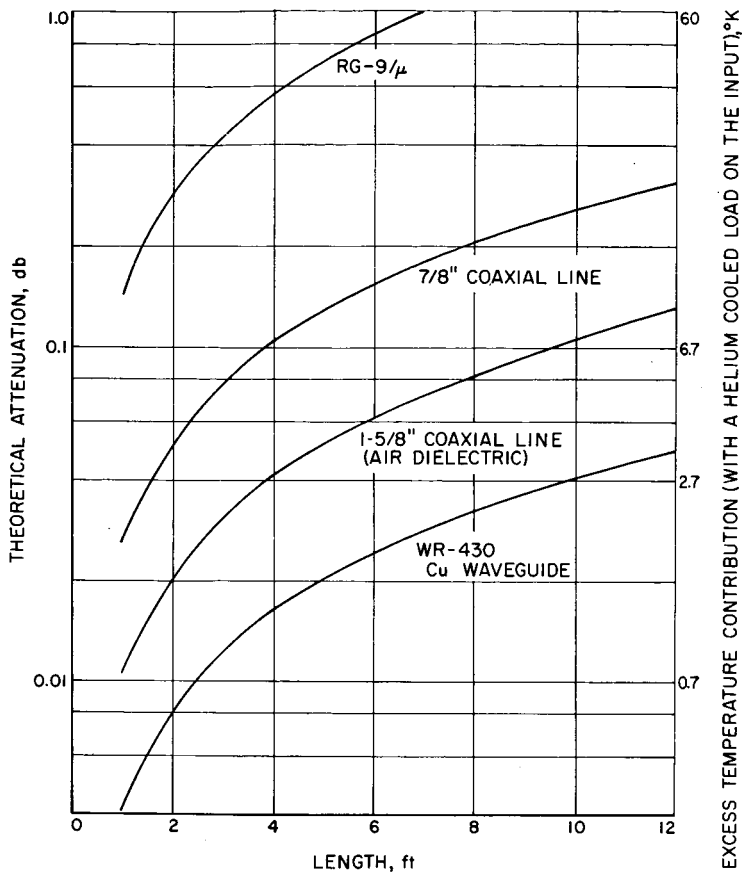
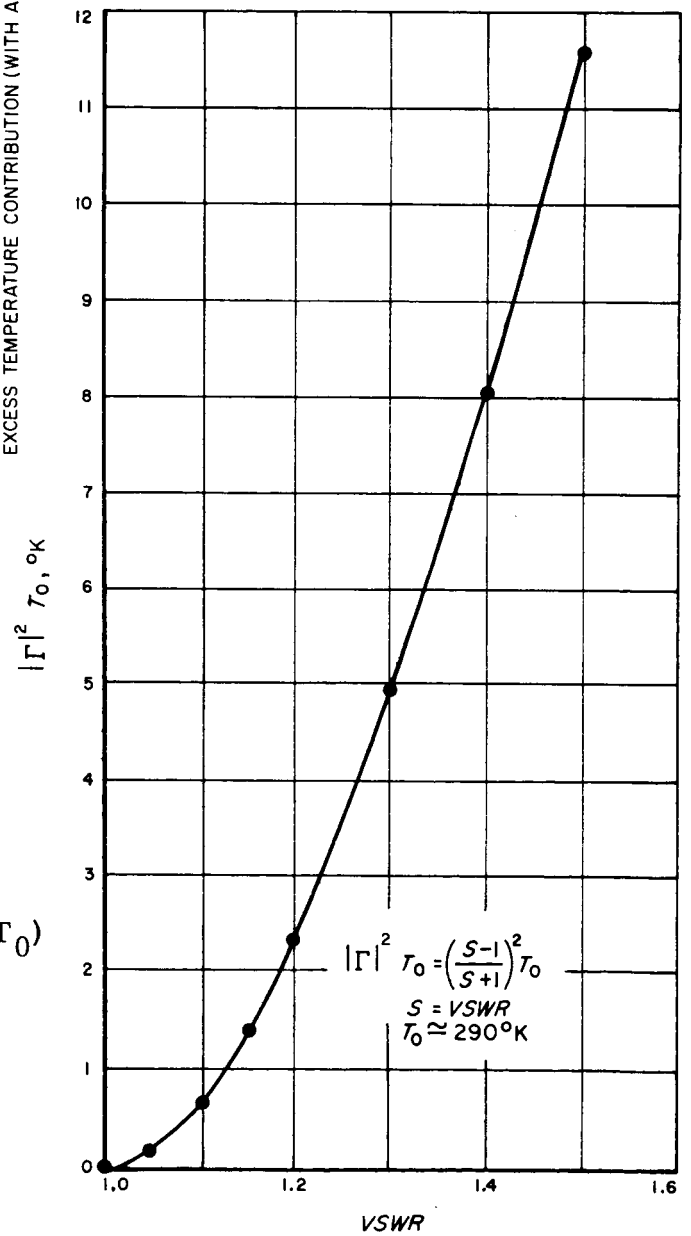


Fig. 3. Transmission lines

Fig. 4. Reflected excess temperature ( $|\Gamma|^2 T_0$ )

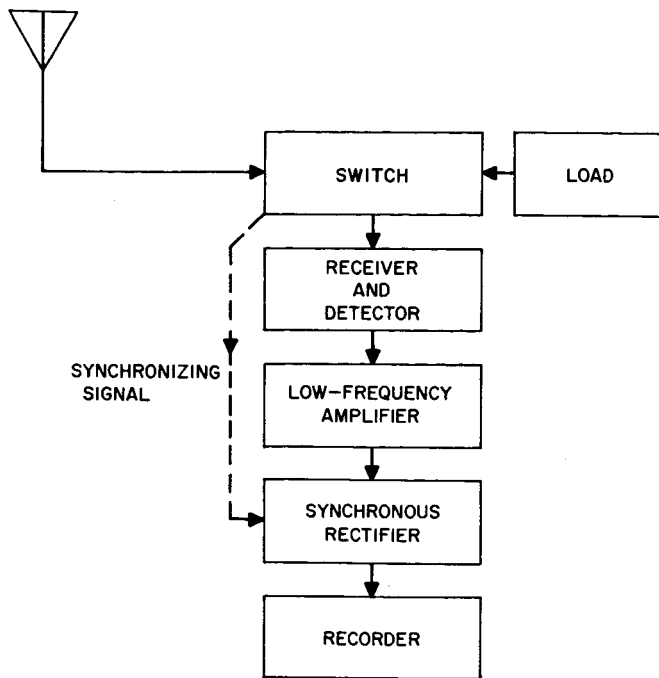


Fig. 5. Simplified diagram of a Dicke radiometer

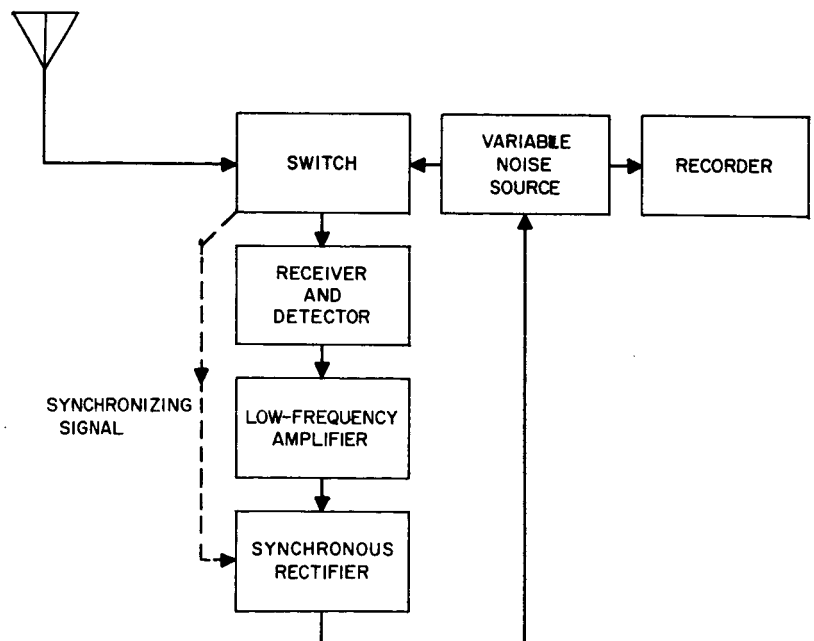


Fig. 6. Simplified diagram of a Ryle and Vanberg radiometer

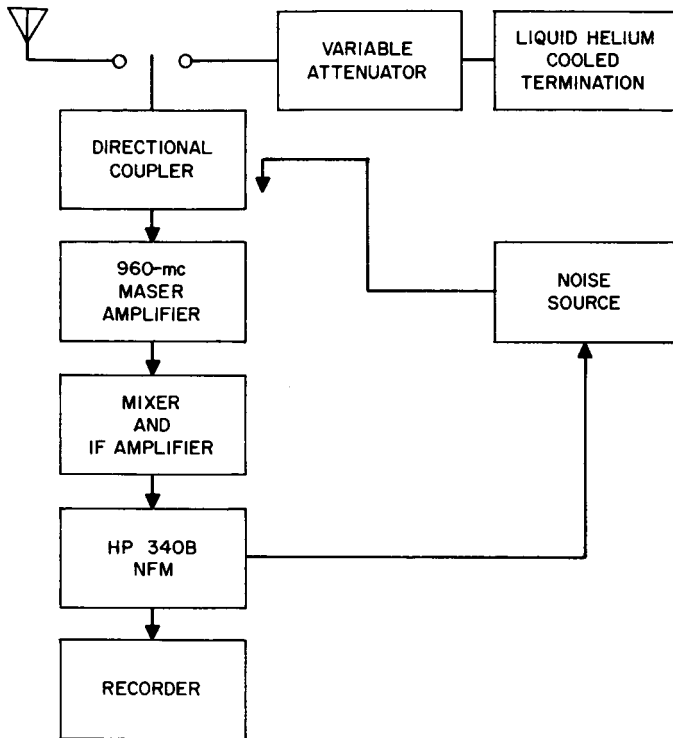


Fig. 7. JPL HA-DEC site maser installation used to measure absolute antenna temperature at 960 mc

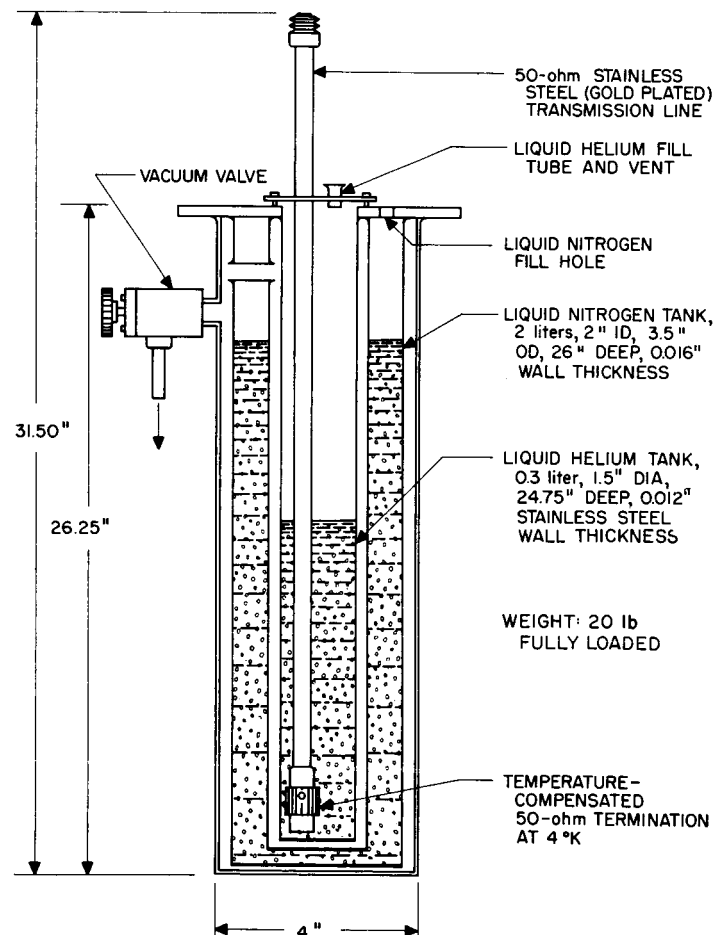


Fig. 8. Liquid helium load (960 mc)

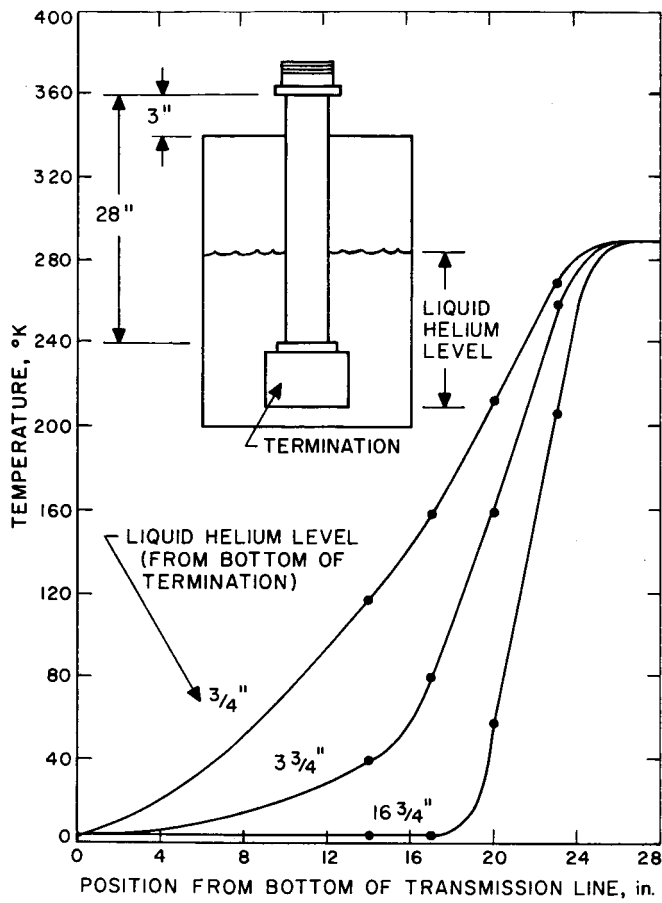


Fig. 9. Temperature distribution along transmission line (960 mc)

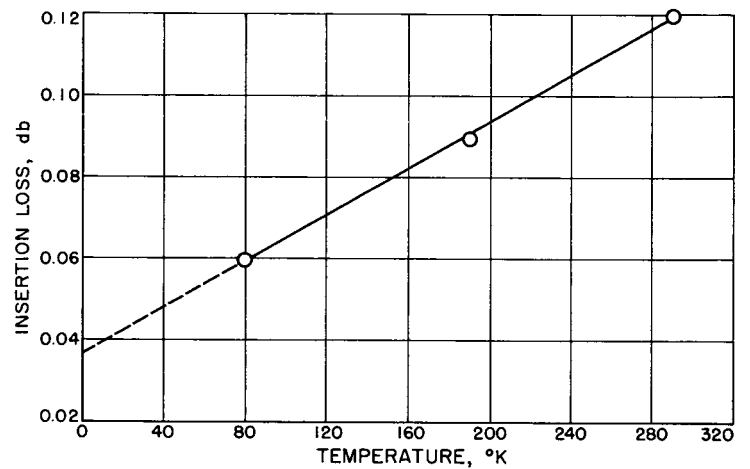
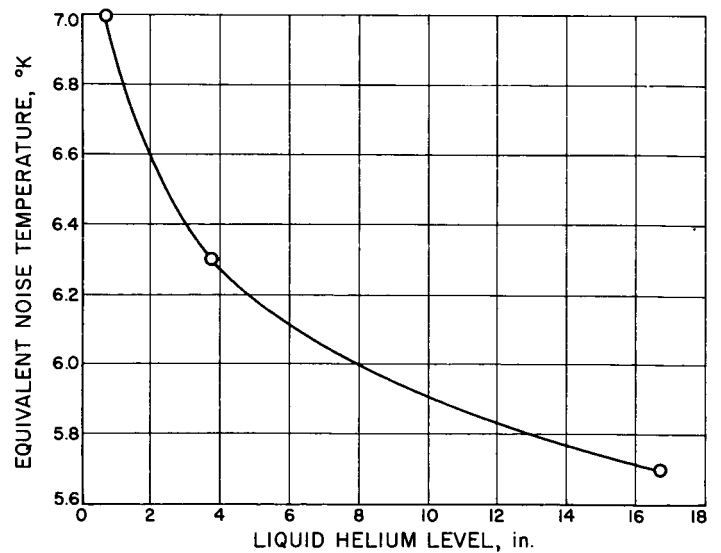


Fig. 10. Insertion loss of transmission line as a function of temperature (960 mc)

Fig. 11. Equivalent noise temperature of helium load as a function of liquid helium level (960 mc)



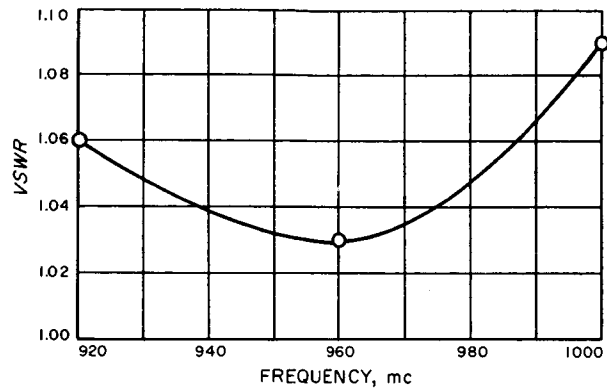


Fig. 12. Plot of VSWR frequency of liquid helium cooled coaxial termination

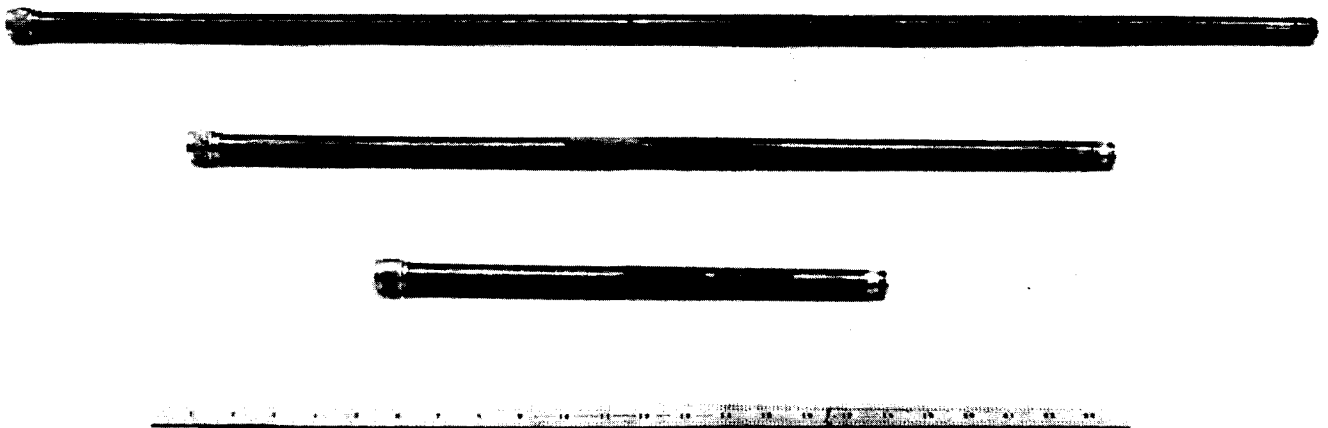


Fig. 13. Precision low-value coaxial attenuators constructed from commercial stainless-steel tubing

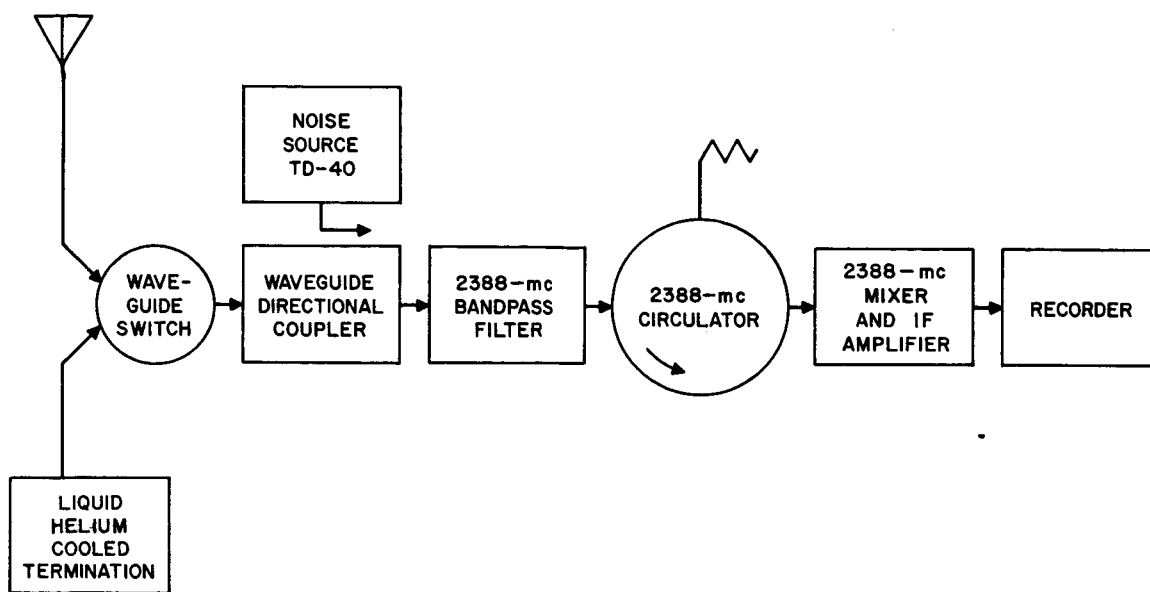


Fig. 14. 2388-mc antenna-temperature measurement setup

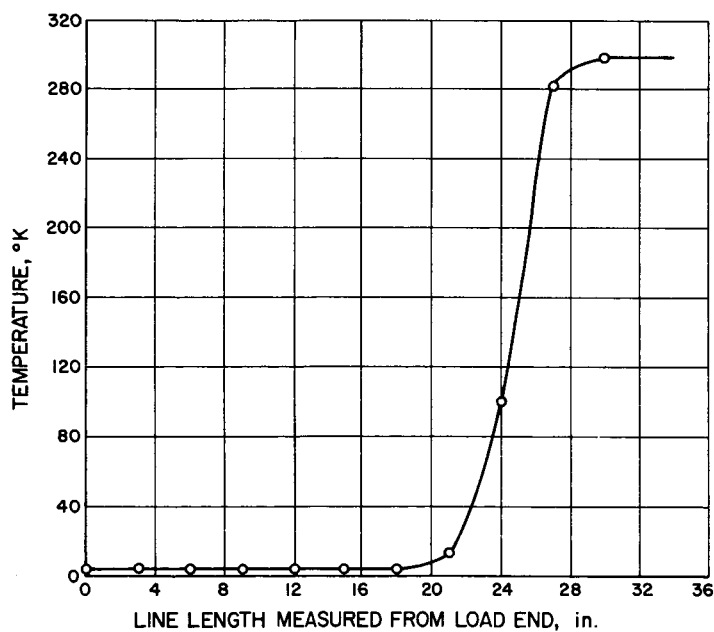


Fig. 15. Temperature distribution along helium load transmission line

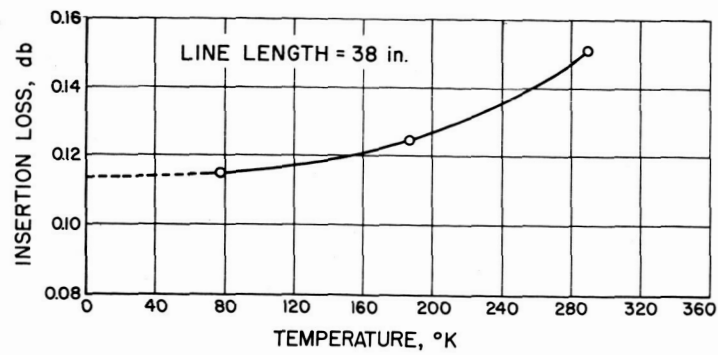


Fig. 16. Insertion loss of 3/4-in. transmission line vs temperature

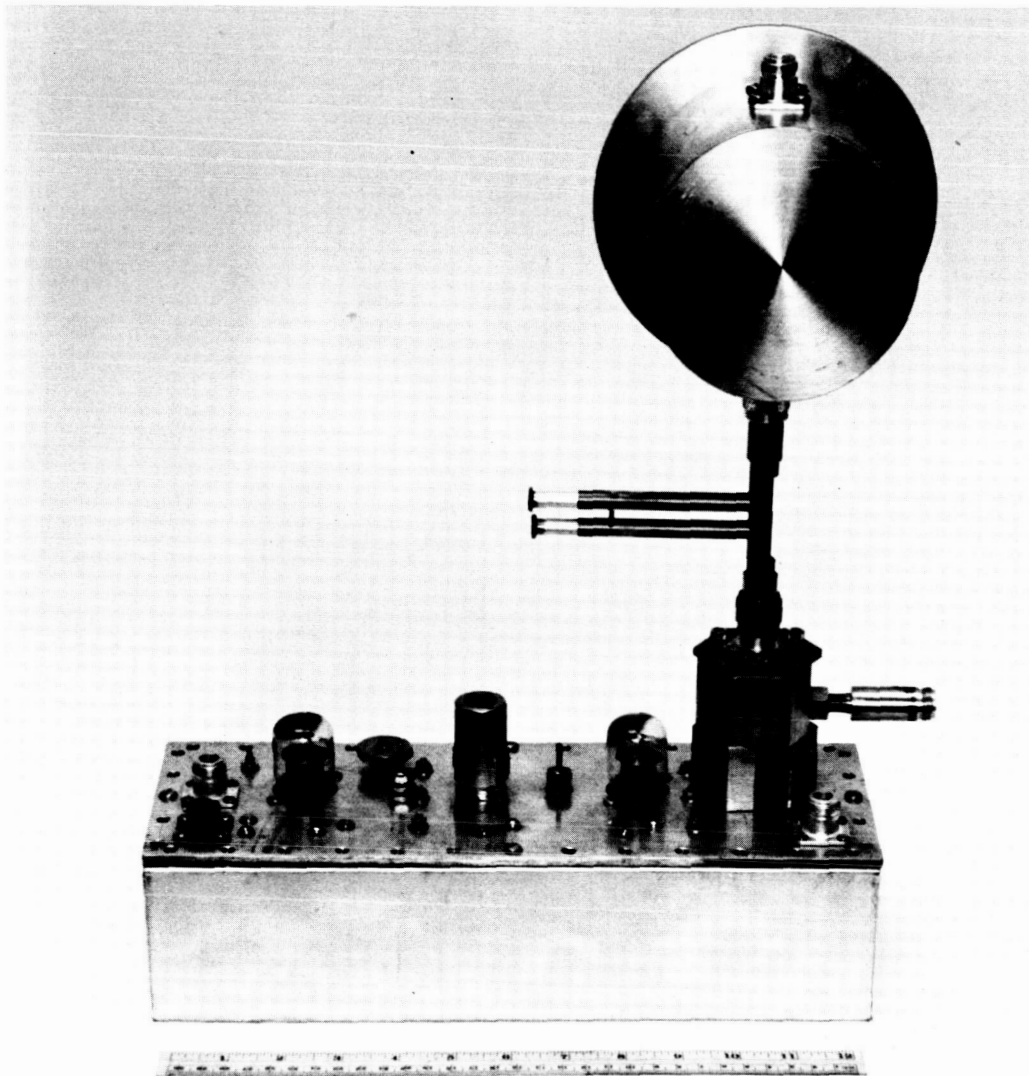


Fig. 17. 2388-mc mixer and 30-mc IF amplifier with bandpass filter and tuner

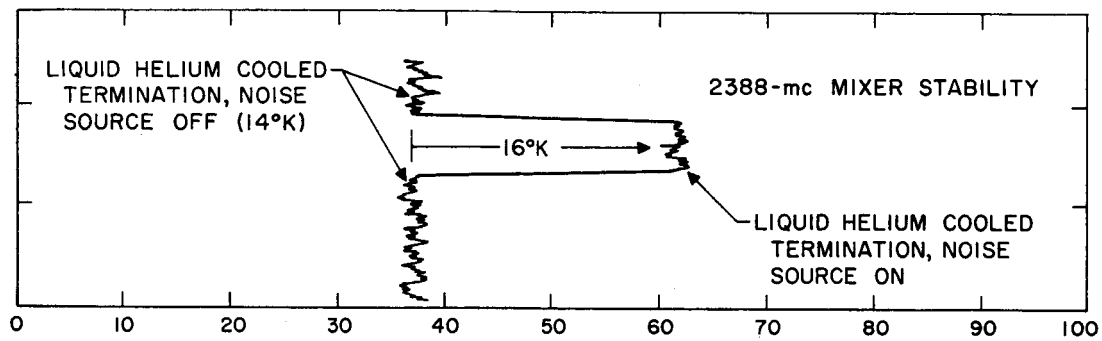


Fig. 18. Recording of detected noise level of 2388-mc mixer

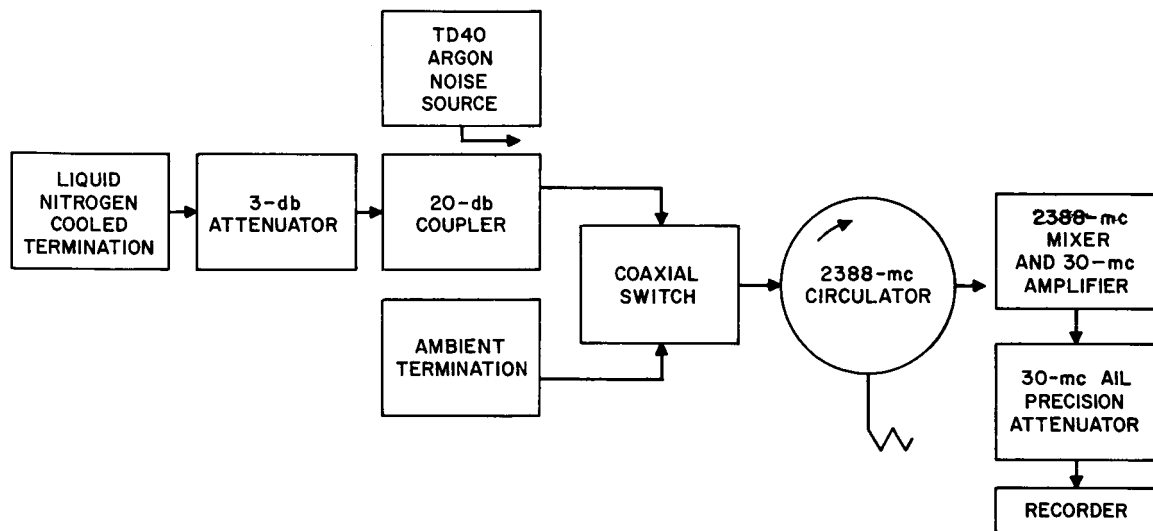


Fig. 19. Noise-source evaluation setup



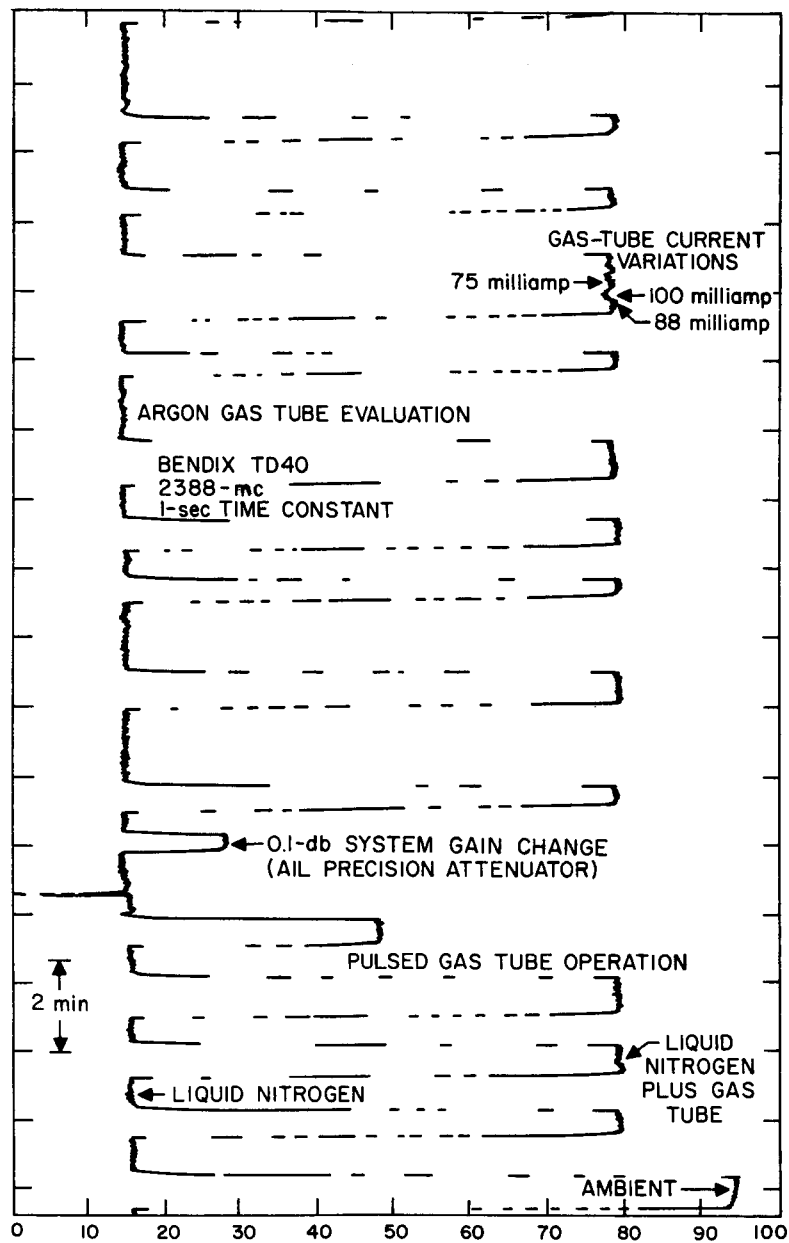


Fig. 20. Recording of excess noise of argon TD40 noise source at 2388 mc

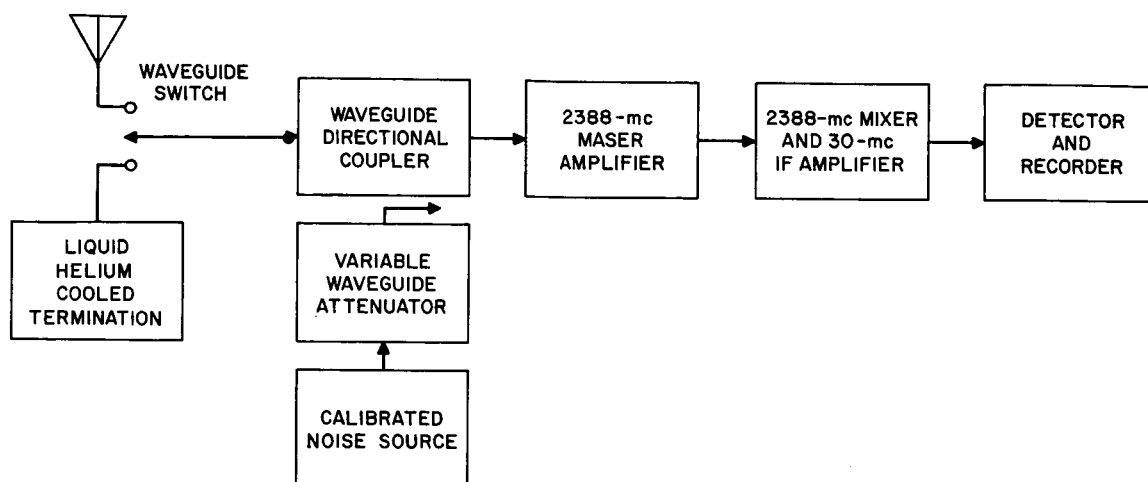


Fig. 21. Radiometer setup using 2388-mc maser amplifier

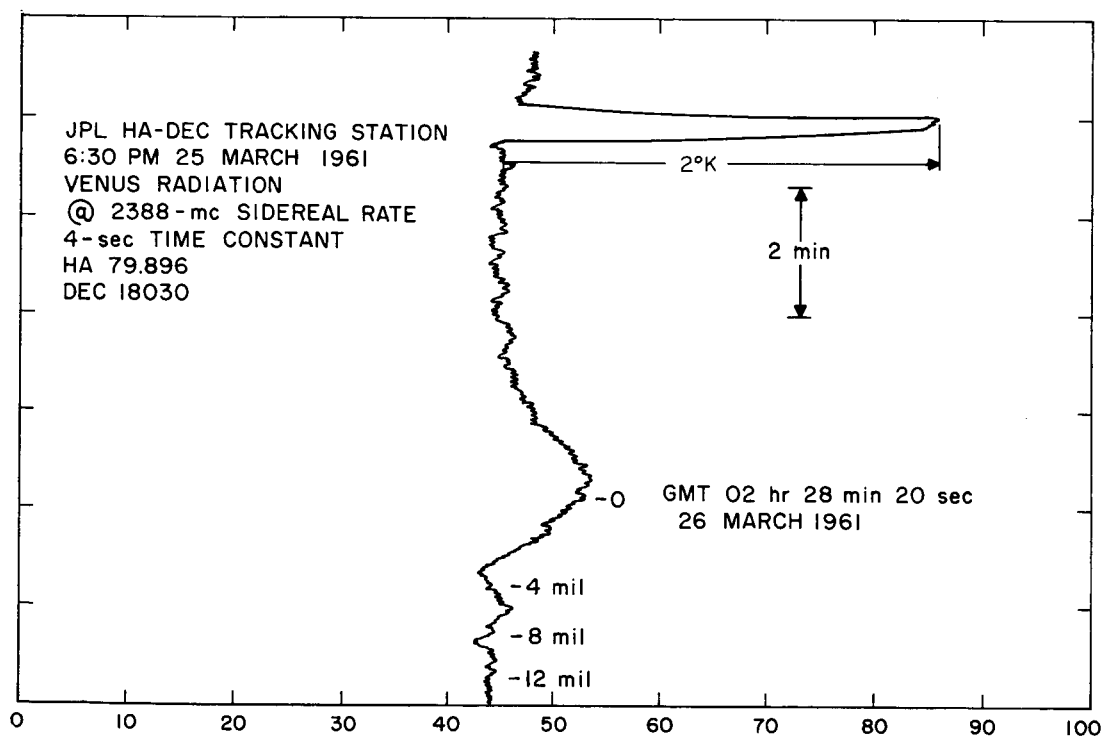


Fig. 22. 2388-mc radiation-drift curve for Venus

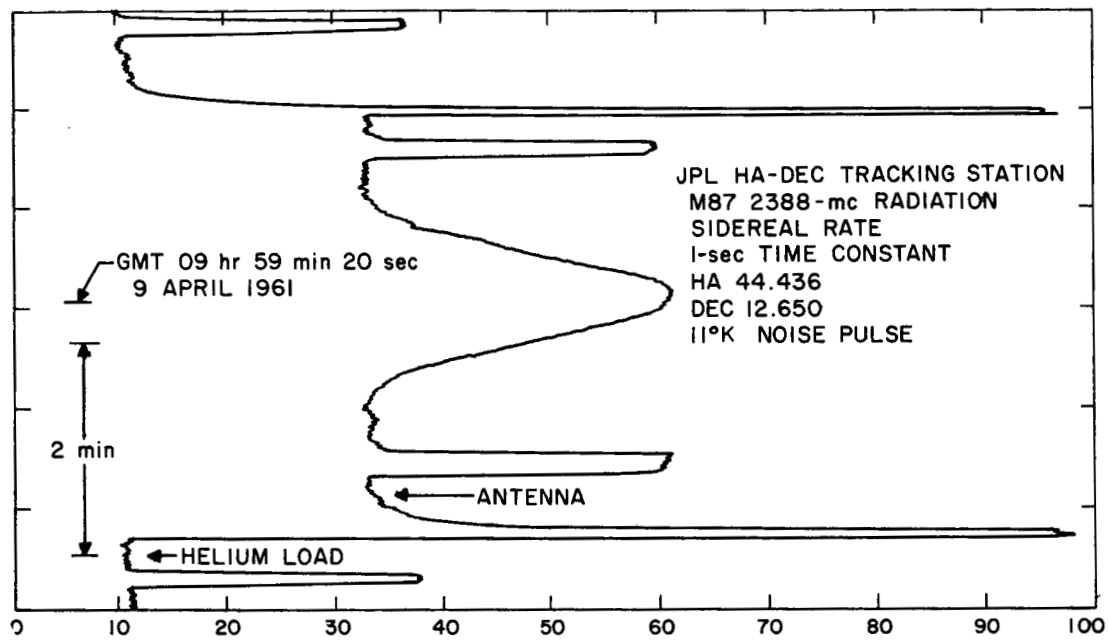


Fig. 23. 2388-mc radiation-drift curve for M87

## REFERENCES

1. Harris, D. E. and Roberts, J. A., "Radio Source Measurements at 960 mc/s," Publications of the Astronomical Society of the Pacific, Vol. 72, No. 427, August 1960, p. 237.
2. Pawsey, J. L. and Bracewell, R. N. Radio Astronomy, Oxford at the Clarendon Press, 1955.
3. Dicke, R. H., Berringer, R., Kyle, R. L., and Vane, A. B., "Atmospheric Absorption Measurements With a Microwave Radiometer," Physical Review, Vol. 70, Nos. 5 and 6, September 1 and 15, 1946, p. 340.
4. Brown, R. H. and Lovell, A. C. B. The Exploration of Space by Radio, John Wiley and Sons, 1958.
5. Stelzried, C. T., "Liquid Helium Cooled Coaxial Termination," Transactions of the IRE (to be published).
6. Research Summary No. 36-6, Vol. I, Jet Propulsion Laboratory, Pasadena, California, December 20, 1960.
7. Research Summary No. 36-8, Vol. I, Jet Propulsion Laboratory, Pasadena, California (to be published).